Uncertainty in preindustrial abundance of tropospheric ozone: Implications for radiative forcing calculations

Citation
Mickley, Loretta J., Daniel J. Jacob, and David Rind. 2001. "Uncertainty in Preindustrial Abundance of Tropospheric Ozone: Implications for Radiative Forcing Calculations." Journal of Geophysical Research 106, issue D4: 3389-3399.

Published Version
doi:10.1029/2000JD900594

Permanent link
http://nrs.harvard.edu/urn-3:HUL.InstRepos:14117812

Terms of Use

Share Your Story

Uncertainty in preindustrial abundance of tropospheric ozone: Implications for radiative forcing calculations

Loretta J. Mickley and Daniel J. Jacob

Division of Engineering and Applied Sciences and Department of Earth and Planetary Sciences
Harvard University, Cambridge, Massachusetts

David Rind

Goddard Institute for Space Studies, New York, New York

Abstract. Recent model calculations of the global mean radiative forcing from tropospheric ozone since preindustrial times fall in a relatively narrow range, from 0.3 to 0.5 W m^{-2}. These calculations use preindustrial ozone fields that overestimate observations available from the turn of the nineteenth century. Although there may be calibration problems with the observations, uncertainties in model estimates of preindustrial natural emissions must also be considered. We show that a global three-dimensional model of tropospheric chemistry with reduced NO$_x$ emissions from lightning (1-2 Tg N yr^{-1}) and soils (2 Tg N yr^{-1}) and increased emissions of biogenic hydrocarbons can better reproduce the nineteenth century observations. The resulting global mean radiative forcing from tropospheric ozone since preindustrial times is 0.72-0.80 W m^{-2}, amounting to about half of the estimated CO$_2$ forcing. Reduction in the preindustrial lightning source accounts for two thirds of the increase in the ozone forcing. Because there is near-total titration of OH by isoprene in the continental boundary layer of the preindustrial atmosphere, isoprene and other biogenic hydrocarbons represent significant ozone sinks. The weak or absent spring maximum in the nineteenth century observations of ozone is difficult to explain within our understanding of the natural ozone budget. Our results indicate that the uncertainty in computing radiative forcing from tropospheric ozone since preindustrial times is larger than is usually acknowledged.

1. Introduction

Ozone in the troposphere is an important greenhouse gas which absorbs both upwelling terrestrial radiation and downwelling solar radiation. It is produced by photochemical oxidation of CO and hydrocarbons in the presence of NO$_x$ (NO+NO$_2$). Anthropogenic emissions of these ozone precursors have led to large increases in tropospheric ozone over the past century [*Marenco et al.*, 1994; *Wang and Jacob*, 1998]. Recent model calculations of the global mean radiative forcing due to tropospheric ozone since preindustrial times fall in the narrow range of 0.3-0.5 W m^{-2}, implying some confidence in our evaluation of the contribution of ozone to climate change [*Ramaswamy*, 2001]. There is, however, considerable uncertainty regarding ozone levels in preindustrial times, here defined as the turn of the nineteenth century. The models calculate changes in the global tropospheric ozone burden from preindustrial times of 7-13 Dobson units (DU, 1 DU = 2.7 × 10^{16} molecules cm^{-2}), in relatively good agreement with each other [*Prather and Ehhalt*, 2001], but they overestimate systematically the late nineteenth and early twentieth century observations available in surface air and at mountain sites [*Wang and Jacob*, 1998]. Observations at Montsouris in Paris, which are considered the most reliable, are 7-10 ppb with little seasonal variation [*Volz and Kley*, 1988]. By comparison, the global models calculate preindustrial surface ozone concentrations over Europe of typically 15-20 ppb [*Roelofs et al.*, 1997; *Brasseur et al.*, 1998a; *Wang and Jacob*, 1998; *Mickley et al.*, 1999; *Kiehl et al.*, 1999]. Comparison with Pic du Midi nineteenth century observations in the free troposphere over France indicates even larger differences [*Wang and Jacob*, 1998]. In a sensitivity study that illustrates the dependence of radiative forcing calculations on the assumed preindustrial ozone, *Kiehl et al.* [1999] set preindustrial ozone everywhere in the troposphere to 5 ppb and obtained a forcing of 1.55 W m^{-2}, comparable to that of CO$_2$ and considerably higher than the conventional value.

The discrepancies between models and observations of ozone in the preindustrial troposphere could possibly reflect calibration problems in the observations [*Kley et al.*, 1988; *Pavelin et al.*, 1999]. However, deficiencies in our ability to simulate preindustrial ozone must also be acknowledged. Aside from CH_4, for which ice core data are available, the preindustrial concentrations of ozone precursors are poorly constrained. Natural sources of ozone precursors include lightning (NO_x), soils, vegetation, and natural fires. Present-day estimates of natural soil NO_x emissions (excluding fertilized agriculture) range from 4 to 13 Tg N yr^{-1} [*Yienger and Levy*, 1995; *Davidson and Kingerlee*, 1997; *Mickley et al.*, 1999], estimates of lightning NO_x emissions range from 2 to 20 Tg N y^{-1} [e.g., *Levy et al.*, 1996; *Price et al.*, 1997; *Huntreiser et al.*, 1998; *Lawrence et al.*, 1999], and estimates of isoprene emissions from vegetation range from 220 to 600 Tg C yr^{-1} [*Guenther et al.*, 1995; *Brasseur et al.*, 1998b; *Wang et al.*, 1998a; *Granier et al.*, 2000]. For the preindustrial atmosphere the uncertainties in these emissions are even larger, given our lack of knowledge of the effect of decades of elevated nitrogen deposition to soils, the influence of anthropogenic aerosols and global warming on lightning intensity, and changes in vegetation type and extent.

In this study we explore to what extent uncertainties in natural sources for the nineteenth century can accommodate the low levels of ozone observed, and we examine the consequences of these uncertainties for radiative forcing assessments. Our research builds on previous work by *Mickley et al.* [1999], in which the radiative forcing of ozone was calculated using a three-dimensional general circulation model, the Goddard Institute for Space Studies general circulation model (GISS GCM) II′ [*Rind and Lerner*, 1996; *Rind et al.*, 1999]. This model contains a detailed description of ozone-NO_x-hydrocarbon photochemistry and standard schemes for emissions of NO_x, hydrocarbons, and CO from natural and anthropogenic sources [*Wang et al.*, 1998a; *Horowitz et al.*, 1998; *Mickley et al.*, 1999]. In the previous study the natural emissions of ozone precursors were the same for the preindustrial and present-day simulations, and biomass-burning emissions in the preindustrial atmosphere were scaled to 10% of their current value. Figures 1a and 1b show the calculated zonally averaged, annual mean ozone for the present-day and preindustrial atmospheres, respectively. The global mean forcing obtained for anthropogenic ozone was 0.44 W m^{-2}, typical of the current generation of models. Using the same model but varying the natural emissions, we now attempt to reproduce the low ozone concentrations reported for the late 1800s and early 1900s, and we recalculate the forcing due to the change in ozone obtained with these scenarios.

Section 2 of this paper briefly describes the *Mickley et al.* [1999] model. In section 3 we scrutinize the model overestimate of the 1870-1910 observations, and
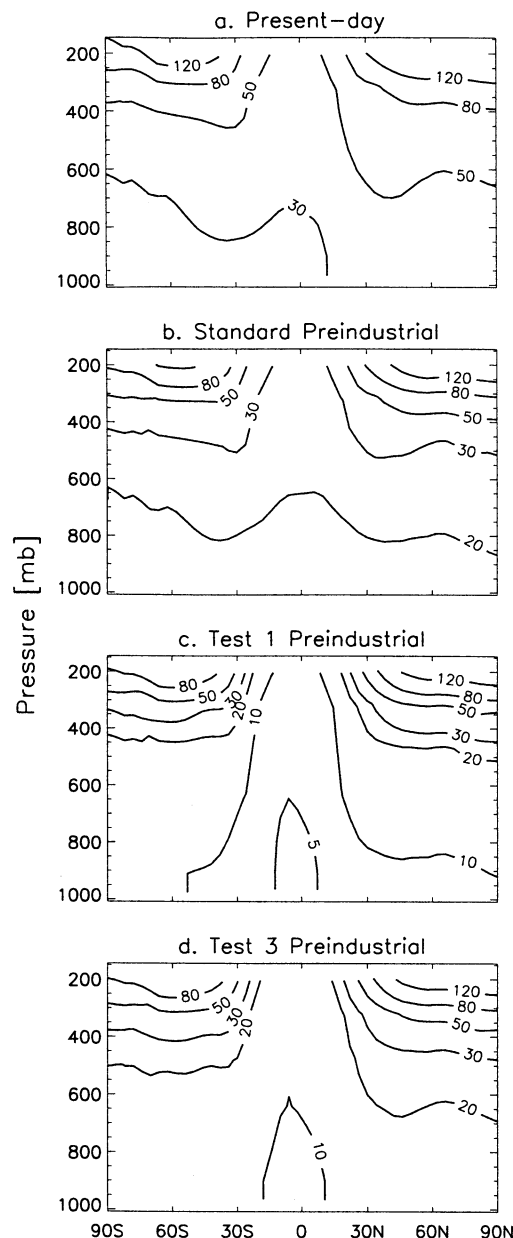

Figure 1. Zonally averaged, annual mean ozone concentration (ppb) calculated by the model as a function of latitude and pressure for (a) the present-day atmosphere, (b) the standard preindustrial atmosphere, (c) the test 1 preindustrial atmosphere, with decreased soil and lightning NO_x emissions and increased emissions from biogenic hydrocarbons, and (d) the test 3 preindustrial atmosphre, with decreased lightning NO_x emissions only.

in section 4 we discuss how these overestimates could possibly reflect uncertainties in the preindustrial emissions of NO_x and nonmethane hydrocarbons. Section 5 presents the results from two test simulations for the preindustrial atmosphere with modified natural emissions. Section 6 reexamines the observations in light of the model results, and section 7 contains our conclusions.

2. Model Description

We use the GISS GCM II' of *Rind and Lerner* [1996] and *Rind et al.* [1999] with embedded capability for on-line simulation of tropospheric ozone-NO_x-hydrocarbon chemistry [*Mickley et al.*, 1999]. The model has a horizontal resolution of 4° latitude and 5° longitude, with nine vertical layers in a sigma coordinate system extending from the surface to 10 hPa. There are 24 tracers transported in the model, including five nonmethane hydrocarbons (ethane, propane, $\geq C_4$ alkanes, $\geq C_3$ alkenes, isoprene) and their oxidation products. For the present-day simulation, methane is set throughout the troposphere at 1.7 ppm. The chemical mechanism includes 80 species (following *Horowitz et al.* [1998], with minor updates) and is integrated over a 4-hour time step. Wet deposition of HNO_3 and H_2O_2 is carried out via the scheme of *Koch et al.* [1999], and dry deposition is computed with a resistance-in-series scheme [*Wang et al.*, 1998a]. The schemes for biogenic and industrial emissions largely follow those of *Wang et al.* [1998a]. In particular, the model follows the algorithm of *Yienger and Levy* [1995] for natural soil NO_x emissions and the algorithm of *Guenther et al.* [1995] for isoprene emission from vegetation. Biogenic emissions of alkenes and acetone are scaled to those of isoprene. The calculation of lightning NO_x emissions is based on *Price and Rind* [1992]. The fluxes of stratospheric ozone and reactive nitrogen into the troposphere are specified as upper boundary conditions at 150 hPa [*Wang et al.*, 1998a]. Table 1 summarizes the natural emission fluxes in the model.

Mickley et al. [1999] evaluated the model simulation for the present-day atmosphere by comparing model results to long-term measurements of ozone and CO, and to aircraft measurements of NO, HNO_3, peroxyacetyl nitrate (PAN), and H_2O_2. At most sites the model captures the monthly mean ozone within about 10 ppb and the seasonal variation within about 1 month. CO concentrations are reproduced by the model within 10 ppb at most sites. Agreement is good between modeled and measured NO, and PAN and H_2O_2 are reproduced within a factor of 2. As in other global three-dimensional models [e.g., *Wang et al.*, 1998b; *Lawrence and Crutzen*, 1998; *Hauglustaine et al.*, 1998], the model overestimates HNO_3 in the remote troposphere by factors of 2 to 3.

The standard preindustrial simulation excludes all anthropogenic emissions, except for biomass burning, which is set to 10% of its current value. Methane is specified at 0.7 ppm. Natural emissions of NO_x, nonmethane hydrocarbons, and CO are the same as for the present day. Soil NO_x emissions from application of fertilizer are turned off. The same meteorological fields and stratospheric ozone fluxes are used as for the present-day simulation.

The radiative heating calculations that drive the GCM meteorology use prescribed, climatological distributions of ozone [*Hansen et al.*, 1983]. To determine the radiative forcing due to anthropogenic ozone, we apply the GCM radiative transfer code to the calculated ozone distributions for the present and preindustrial atmospheres, and compare the shortwave and longwave fluxes at the tropopause. The forcings we calculate in this way are instantaneous forcings.

3. Results from the Standard Preindustrial Simulation

Results from the standard preindustrial simulation were presented previously by *Mickley et al.* [1999], who

Table 1. Natural Emission Fluxes in the Model[a]

	Standard	Test 1	Test 2	Test 3
NO_x				
Soil	3.9	2.0	2.0	3.9
Lightning	3.5	1.0	2.0	1.0
Biomass burning	1.1	1.1	1.1	1.1
Stratosphere	0.1	0.1	0.1	0.1
CO				
Biomass burning	51	51	51	51
Isoprene				
Vegetation	550	825	825	550
Monoterpenes[b]				
Vegetation	0	200	200	133
$\geq C_3$ alkenes				
Vegetation	16	24	24	16
Biomass burning	1.2	1.2	1.2	1.2
Acetone				
Vegetation	14	21	21	14

[a]Units are Tg N yr^{-1} for NO_x, Tg CO yr^{-1} for CO, and Tg C yr^{-1} for the other molecules. Values are global annual means.

[b]Emitted as half α-pinene, half β-pinene.

found a global burden of ozone of 230 Tg, compared to 360 Tg for the present day (Table 2). The change in ozone yields a global mean radiative forcing of 0.44 W m^{-2} (0.35 longwave + 0.09 shortwave).

Figure 2 compares late nineteenth century and early twentieth century observations of ozone to results from the standard preindustrial model at 12 sites worldwide [*Volz and Kley*, 1988 ; *Marenco et al.*, 1994; *Pavelin et al.*, 1999]. Except for Pic du Midi (3.0 km) and Mont Ventoux (1.9 km), the sites are less than 0.5 km in elevation. At all sites the model overestimates ozone by 5-15 ppb. The model peaks in winter-spring, when ozone transport from the stratosphere is maximum and photochemical loss in the troposphere is slow. At most sites the observed seasonal cycle is in phase with, but much weaker than, that calculated by the model. At three sites (Luanda, Mont Ventoux, and Montsouris), almost no seasonal variation was observed.

How reliable are the preindustrial measurements of ozone? In reconstructing these early observations of surface ozone, interferences had to be taken into account, and for all of the sites except Montsouris, calibration of the measurements needed to be done. Both correcting for interferences and calibration introduce uncertainty. For example, *Bojkov* [1986] in his study of preindustrial ozone corrected the Montsouris data for formaldehyde, while *Volz and Kley* [1988] corrected the same data set for SO$_2$. *Volz and Kley* [1988] also excluded observations made at Montsouris when the wind blew across Paris, carrying SO$_2$ and other interfering gases. Calibration of the measurements other than at Montsouris involves converting a colorimetric scale to mixing ratio and is not straightforward [e.g., *Marenco et al.*, 1994; *Pavelin et al.*, 1999]. The measurement method at these sites, known as the Schönbein method, utilizes strips of blotting paper soaked in a potassium iodide solution and exposed to air. In general, the observations at Montsouris are thought to be the most reliable since they relied on a quantitative method involving the oxidation of arsenate in solution [*Kley et al.*, 1988].

Some of the model overestimate may be caused by inability to resolve the nighttime deposition of ozone in a shallow stable surface layer, as the lowest model layer is about 500 m deep. The preindustrial ozone measurements, typically collected over the day and night, would be affected by this nighttime deposition. *Logan* [1989], however, found only a 25% diurnal variation in present-day ozone at rural surface sites in the United States. *Volz and Kley* [1988] discarded from the Montsouris data set any measurements made during stagnant periods (wind speed less than 1 km h^{-1}), when local dry deposition of ozone would be especially important. In any case, nighttime deposition would not play a role at the mountain sites of Pic du Midi and Mont Ventoux.

A problem common to all sites except Montsouris is that at long exposure times the Schönbein measurements may not be proportional to the total dose of ozone [*Kley et al.*, 1988], leading to underestimates of ozone. The problem could help explain the low values and damped seasonal cycle of ozone observed at most of the sites, but it cannot account for the low values observed at Montsouris.

A striking feature of the continental boundary layer chemistry in the model preindustrial atmosphere is the near-complete titration of OH by isoprene, both at midlatitudes and the tropics. The model computes isoprene mixing ratios 2-5 times greater in the preindustrial boundary layer over continents than those in the present-day boundary layer; concentrations of OH are

Table 2. Calculated Global Radiative Forcing Since Preindustrial Times Due to Tropospheric Ozone[a]

	Preindustrial			
	Standard	Test 1[b]	Test 2[c]	Test 3[d]
Burden,[e] Tg O$_3$	230	136	160	175
Change in O$_3$, DU	12.6	21.1	20.0	18.6
Longwave forcing, W m^{-2}	0.35	0.64	0.57	0.53
Shortwave forcing, W m^{-2}	0.09	0.16	0.15	0.14
Total forcing, W m^{-2}	0.44	0.80	0.72	0.67

[a] All values are global annual averages.

[b] In this simulation, soil NO$_x$ emissions were halved relative to the standard simulation to 2.0 Tg N yr^{-1}; biogenic emissions of isoprene, alkenes, and acetone were increased by 50%; monoterpene emissions were added; and lightning NO$_x$ emissions were decreased to 1.0 Tg N yr^{-1} from 3.6 Tg N yr^{-1}.

[c] This simulation is the same as test 1, except lightning NO$_x$ emissions were decreased to 2.0 Tg N yr^{-1}.

[d] This simulation is the same as the standard simulation, except lightning NO$_x$ emissions were decreased to 1.0 Tg N yr^{-1} as in test 1.

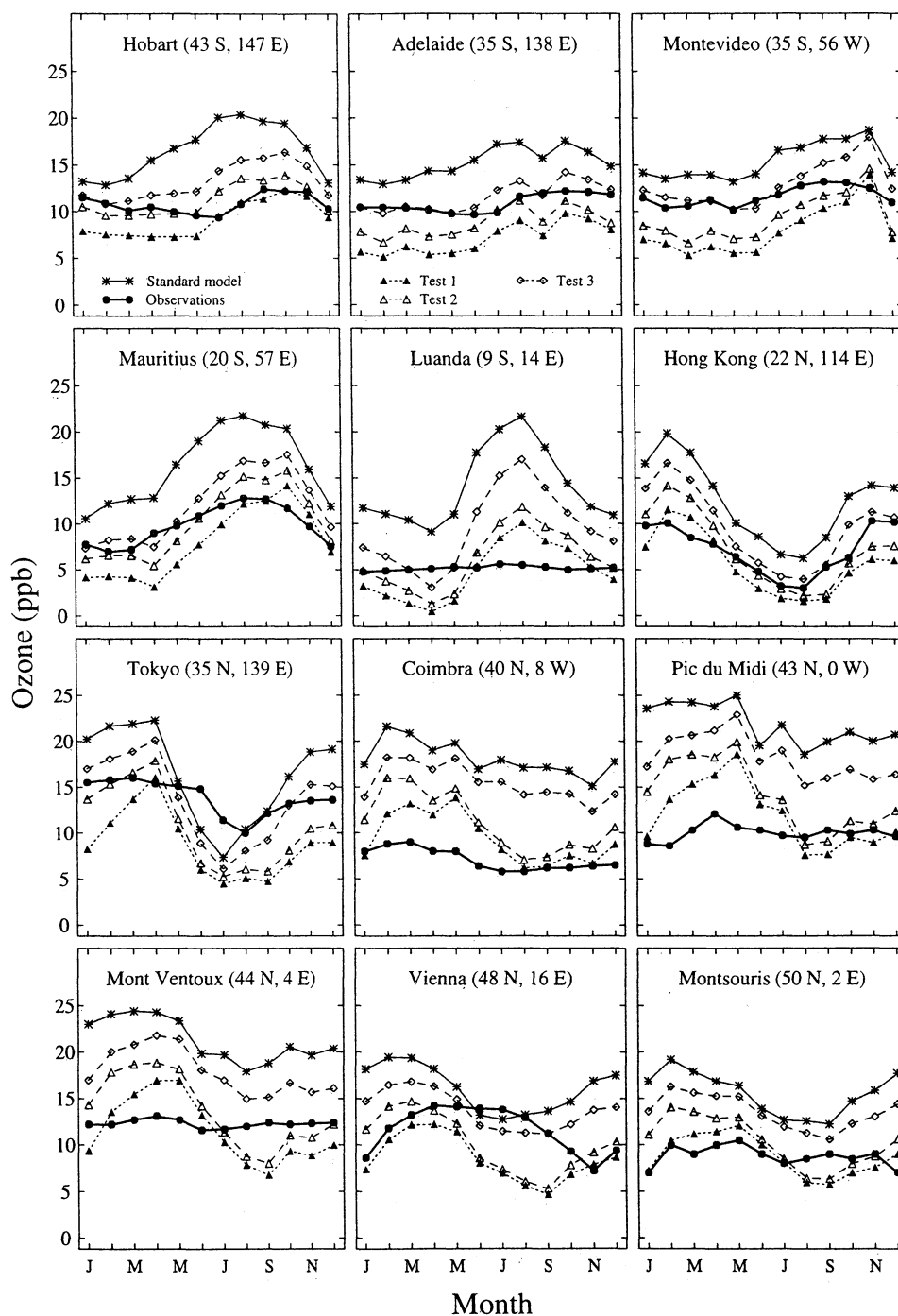[e] For comparison, the global burden for the present-day simulation is 360 Tg.

Figure 2. Simulated preindustrial ozone concentrations (ppb) in surface air, compared to 1870-1910 observations at sites throughout the world. The observations are shown as solid circles connected with a heavy line. The Pic du Midi data (1874–1884) are from *Marenco et al.* [1994]; the Montsouris data (1876–1886) are from *Volz and Kley* [1988], and all other sites (late 1800s to early 1900s) are from *Pavelin et al.* [1999]. Except for Pic du Midi (3.0 km) and Mont Ventoux (1.9 km), the sites are less than 0.5 km in elevation. The results from the standard preindustrial simulation are shown as connected stars. Results from the test 1 simulation (with decreased soil NO_x emissions, lightning NO_x emissions scaled to 1.0 Tg N yr^{-1}, and increased emissions from biogenic hydrocarbons) are connected solid triangles. Results from the test 2 simulation, which is the same as the test 1 simulation but with lightning NO_x emissions scaled to 2.0 Tg N yr^{-1}, are connected open triangles. Results from the test 3 simulation, with only lightning NO_x emissions changed to 1.0 Tg N yr^{-1}, are connected diamonds. Model results for Pic du Midi and Mont Ventoux were sampled at the appropriate altitude.
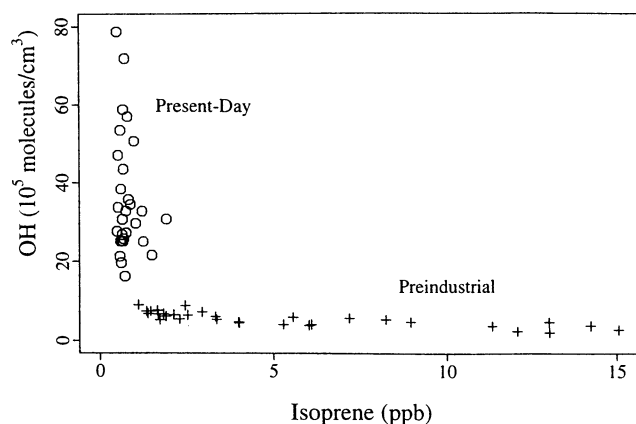
Figure 3. Calculated OH concentrations (molecules cm^{-3}) versus isoprene mixing ratios (ppb) for noontime conditions in July at Montsouris in Paris. The crosses represent results for the preindustrial simulation, and the circles represent results for the present-day simulation.

less than 20% of present-day values. Figure 3 shows noontime OH concentrations versus isoprene for the standard preindustrial and present-day simulations at Montsouris during the month of July. In the present-day atmosphere, surface OH is usually present in sufficient quantities at the surface to control isoprene [e.g., *Jacob and Wofsy*, 1988]. In the low-NO$_x$ preindustrial atmosphere, in which less OH is recycled by peroxy + NO reactions, isoprene emissions usually titrate OH. The chemical lifetime of isoprene in the boundary layer in July in the preindustrial calculation is about 1 day, more than 4 times its lifetime in the present-day simulation, and sufficient to allow significant transport of isoprene to the free troposphere.

The combination of high levels of isoprene together with low levels of OH has consequences for the preindustrial ozone budget. Ozone competes with OH for reaction with isoprene and the other biogenic hydrocarbons. For the present-day atmosphere, oxidation by ozone accounts for only 15% of isoprene loss; for the standard preindustrial atmosphere it accounts for 30%. Figure 4 shows the rates of the four main ozone loss processes during July for both the preindustrial era and the present day at Montsouris as well as at Luanda, on the west coast of Africa, and Pic du Midi. The rates are for the boundary layer (0-2.6 km), representing the three lowest model layers at Montsouris and Luanda; at Pic du Midi the rates are for 2.6-4.7 km altitude, corresponding to the model layer that contains the mountain peak. The reaction of ozone with isoprene dominates ozone loss at Luanda in the preindustrial simulation. At Montsouris it is of comparable importance to the chemical loss from photolysis (O(^{1}D) + H$_2$O), although less than the loss from deposition. Even at Pic du Midi, in the free troposphere, reaction with isoprene represents about 30% of total ozone loss.

4. Uncertainties in Simulating the Preindustrial Atmosphere

We consider here a number of possible uncertainties in our simulation of the preindustrial atmosphere that could contribute to the ozone overestimates shown in Figure 2. It is unlikely that excessive ozone transport from the stratosphere could be responsible. Our estimate for the present-day stratospheric flux, 390 Tg yr^{-1}, is already at the low end of the values calculated by other models (390-846 Tg yr^{-1} [*Hauglustaine et al.*, 1998]). *McLinden et al.* [2000] estimate a present-day flux of 475 Tg yr^{-1} on the basis of correlations between ozone and reactive nitrogen in the lower stratosphere. If anything, the cross-tropopause flux of ozone would have decreased over the past decades due to ozone depletion in the stratosphere [*Roelofs et al.*, 1997].

It is likely that soil emission of NO$_x$ was lower in the preindustrial atmosphere. *Vitousek et al.* [1997] estimate that human activity has caused a doubling of the rate of nitrogen input to ecosystems on a global scale as a result of fossil fuel combustion, application of industrial fertilizer, and cultivation of nitrogen-fixing crops. It is well known that application of nitrogen fertilizer for agriculture stimulates soil emission of NO [*Williams et al.*, 1997; *Davidson and Kingerlee*, 1997]. We expect that the "natural" emissions of soil NO$_x$ in current inventories [*Yienger and Levy*, 1995; *Davidson and Kingerlee*, 1997] include an anthropogenic component from inadvertent fertilization. For a test case of the preindustrial simulation, we halve the biogenic source of soil NO$_x$, from 3.9 to 2.0 Tg N yr^{-1}. This reduction is applied as a uniform scaling coefficient over the globe.

The preindustrial emission of biogenic hydrocarbons from vegetation is another source of uncertainty. Biogenic hydrocarbons are an important sink for ozone in the preindustrial atmosphere, as pointed out in the previous section. As noted above, the rate of biogenic hydrocarbon emission is not well known even for the present-day atmosphere [*Guenther et al.*, 1995]. For the preindustrial atmosphere, we must also contend with large uncertainties regarding the extent and type of vegetation. For example, the trend toward deforestation in the tropics in the past century is well documented but not easily quantified [e.g., *Palo*, 1999]. In northern midlatitudes, the trend appears to be in the opposite direction, as forests harvested during the preindustrial era are permitted to regrow [*Mather et al.*, 1999].

For a test preindustrial case, we increase the emissions of biogenic isoprene, alkenes, and acetone by 50% throughout the world. We also implement monoterpene emission and chemistry. Like isoprene, monoterpenes are emitted biogenically and react with both OH and ozone [*Griffin et al.*, 1999], and in the preindustrial simulation the principal sink is reaction with ozone due to depletion of OH. Monoterpenes are inconsequential for ozone in the present-day atmosphere, at least in current models, but they are more important in the preindus-
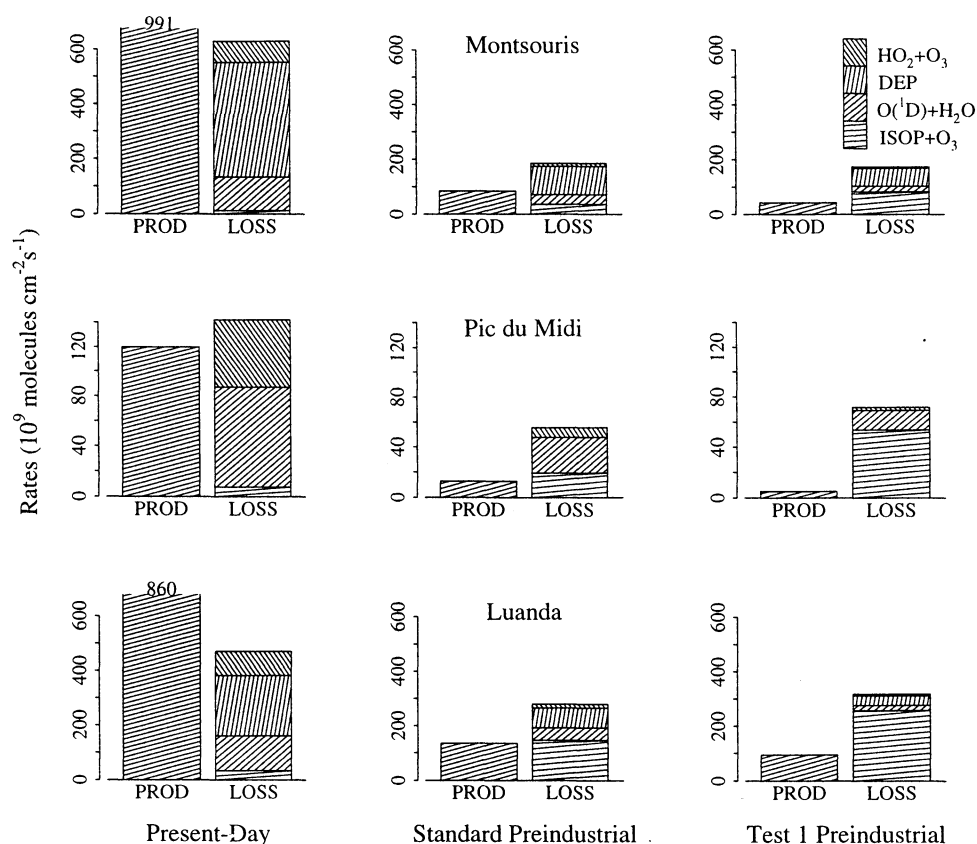
Figure 4. Chemical production and loss rates of ozone in July at three sites where 1870-1910 measurements are available (Figure 2). Values are column rates for the boundary layer (0-2.6 km altitude) except for Pic du Midi, where they are for the 2.6-4.7 km column (hence no deposition sink). Model results are shown for the present-day simulation, standard preindustrial simulation, and preindustrial test 1. PROD includes the ensemble of peroxy + NO reactions producing ozone. Individual loss processes are shown. Note the difference in scales between Pic du Midi and the other sites.

trial atmosphere. We follow the monoterpene emission formulation of *Guenther et al.* [1995], but as with the other biogenic emissions, we increase the standard emissions by 50%, from 133 Tg C yr^{-1} in the *Guenther et al.* [1995] inventory to 200 Tg C yr^{-1}. We assume that all the monoterpenes are emitted as pinenes (half as α-pinene, half as β-pinene), and we describe pinene photochemistry following the mechanism of *Bey* [1997]. In sensitivity studies we find that the main effect of increased biogenic hydrocarbons is to reduce ozone in summer.

The rate of emission of NO_x from lightning is also not well known for the present-day atmosphere, and could have been different in the preindustrial atmosphere. In our standard calculations, we use the same distribution and magnitude of lightning NO_x emissions for both atmospheres. Several studies, however, have proposed a link between aerosol concentrations and lightning frequency. *Lyons et al.* [1998] measured increased cloud-to-ground lightning in air contaminated with smoke from Mexican forest fires. *Westcott* [1995] found that the frequency of cloud-to-ground lightning

increased 40-85% downwind of many cities relative to upwind. In addition, warmer surface temperatures in the present-day atmosphere may have led to increased convection and thus increased lightning frequency, although a GCM simulation by *Price and Rind* [1994] suggests that the effect is less than 5%. For our preindustrial test cases, we use lower limit estimates for the lightning NO_x source of 1.0 and 2.0 Tg N yr^{-1}, with the same distribution as for the present day. A value of 2.0 Tg N yr^{-1} represents the lower bound of current estimates for the lightning source [*Lawrence et al.*, 1999].

It is unlikely that reaction with organic aerosol could constitute an overlooked sink of tropospheric ozone in the preindustrial atmosphere. *Penner* [1995] reports an average organic aerosol concentration at remote sites of about 1.0 μg C cm^{-3} in the present-day atmosphere. If we assume that half the carbon mass is biogenic in origin and use a particle radius of 0.1 μm, a reaction probability of ozone uptake on organic aerosol of 10^{-4} [*De Gouw and Lovejoy*, 1998], and a preindustrial ozone concentration of 10 ppb, we obtain an ozone loss rate

in the boundary layer due to reaction with natural organic aerosol of 8.8×10^9 molecules cm^{-2} s^{-1}. A similar value, 9.2×10^9 molecules cm^{-2} s^{-1}, is computed using a global source strength for biogenic organic aerosol of 88 Tg C yr^{-1} [*Penner*, 1995], assuming that the ratio of double bonds to carbon atoms in the aerosol is 0.1, and further assuming that ozone reacts quantitatively with the available double bonds. These ozone loss rates are small compared to the values shown in Figure 4.

5. Results from the Test Simulations

We performed three test simulations in an effort to reproduce the observed concentrations of ozone from the turn of nineteenth century. In test 1, all the changes described in section 4 were implemented, including a global lightning source of 1.0 Tg N yr^{-1} (Table 1). Test 2 is the same as the test 1, except that the lightning source is 2.0 Tg N yr^{-1}, the lower bound of current estimates [e.g., *Lawrence et al.*, 1999]. Test 3 is the same as the standard simulation except for reduction of the lightning source to 1.0 Tg N yr^{-1}.

Figure 2 shows the results from each test simulation in comparision with the 1870-1910 observations. Results for test 1 generally match or fall below the observations. The discrepancy at most sites is less than 5 ppb. The model results at most sites still show more seasonal variation than the observations. However, the particularly good match between calculated and observed ozone at Montsouris is encouraging given the higher reliability of the measurements there [*Volz and Kley*, 1988]. Figure 4 shows the ozone budget terms for this test case at selected sites for July. Relative to the standard preindustrial simulation, ozone production is reduced by about half, and the lifetime of ozone in the boundary layer is decreased by 25% because of increased loss by reaction with isoprene.

The test 1 case represents our best effort to reproduce the observations of the late 1800s. In Figure 1c, we show the resulting annual mean, zonally averaged ozone concentrations. In the lower troposphere the concentrations range from 5 to 10 ppb, in agreement with observations. The difference between the ozone concentrations in the standard preindustrial simulation and those of the test case ranges from 8 to 10 ppb in the lower troposphere, where soil NO_x and biogenic hydrocargon emissions are important, to about 20 ppb in the tropical upper troposphere, where lightning NO_x emissions play a major role in the ozone budget. For this first test case, we calculate a globally and annually averaged change in ozone column from the preindustrial era to the present day of 22.1 DU, compared to 12.6 DU for the standard case [*Mickley et al.*, 1999].

The global and annual mean total radiative forcing obtained for the test 1 case is 0.80 W m^{-2} (0.64 W m^{-2} in the longwave, 0.16 W m^{-2} in the shortwave), compared to 0.44 W m^{-2} in the standard model. The pat-

tern of the forcing (not shown) resembles that in the standard model [*Mickley et al.*, 1999], with the largest forcings occurring over continents at midlatitudes and low latitudes in the Northern Hemisphere. The maximum forcing in December-January-February over sub-Saharan Africa reaches 1.5 W m^{-2}, or about double that calculated with the standard model [*Mickley et al.*, 1999]. In June-July-August, the greatest forcings, 1.2-2.0 W m^{-2}, appear over the northern midlatitudes to low latitudes, compared to 1.0-1.2 W m^{-2} in the standard case. Averaged over the year, the radiative forcing in the tropics is more than double that of the standard simulation.

The emissions of the test 2 case are the same as in test 1, except that the lightning NO_x source is 2.0 Tg N yr^{-1}. Figure 2 shows the resulting monthly mean ozone concentrations for the 12 observed sites. In the Southern Hemisphere the model results match the observations better than the first test case. At Montsouris during winter, however, the model results overestimate the observed values by about 50%, indicating the sensitivity of midlatitude ozone in the Northern Hemisphere to tropical lightning NO_x emissions at this time of year. This is not surprising given the long lifetime of ozone in winter (weeks to months). For the test 2 case, the annual and global mean change in ozone column from the preindustrial time until the present day is 20.0 DU, which yields a radiative forcing of 0.72 W m^{-2} (0.57 W m^{-2} in the longwave, 0.15 W m^{-2} in the shortwave).

In the test 3 case, only emissions of preindustrial lightning were changed relative to the standard simulation (Table 1). The resulting monthly mean ozone concentrations fall roughly halfway between the test 1 case and the standard preindustrial simulation (Figure 2). The summer minimum at northern midlatitudes is less pronounced than in test 1, where higher biogenic hydrocarbon emissions drive faster ozone loss. In general, the test 3 case overestimates ozone by 5-8 ppb compared to the observations except in summer in the Southern Hemisphere, where it matches the observations better than the first case.

Figure 1d shows the annually averaged, zonal mean concentrations in the test 3 case. The difference between this test case and the standard simulation ranges from a few parts per billion in the lower troposphere to 12 ppb in the upper troposphere. The annual and global mean change in ozone column from preindustrial time to present-day conditions is 18.6 DU. The corresponding radiative forcing is 0.67 W m^{-2} (0.53 W m^{-2} in the longwave, 0.14 W m^{-2} in the shortwave).

Comparing the forcings for the four simulations (the standard simulation and the three tests), we find that the global mean forcing scales linearly with the change in ozone column amount (Table 2). The linear relationship, which has been previously noted [*Houghton et al.*, 1992], indicates that radiative forcing by tropospheric ozone is still far from saturation.

6. A Reexamination of the Observations

One may ask to what extent can any model reproduce the seasonal and spatial variations observed in preindustrial ozone? Put another way, are the preindustrial observations, taken together, consistent with current understanding of the preindustrial ozone budget? Or do model results cast doubt on the reliability of the observations? To answer these questions, we examine the seasonal and spatial variation in the observations.

As noted above, some evidence of the expected spring maximum in ozone can be seen at most sites, especially in the Southern Hemisphere midlatitudes and at Mauritius. These maxima are weaker than those calculated by the model. According to theory, the spring maximum at midlatitudes is due to the longer lifetime of ozone in winter together with increased stratospheric flux of ozone in spring. At Mauritius, at 20°S, about half the spring maximum is due to the influence of biomass burning, and about half is due to the stratospheric flux. Even at 10% of current levels, biomass burning induces a significant seasonal signal on tropical tropospheric ozone. At Tokyo and Hong Kong, the observed ozone levels are flat in winter and spring, but show a minimum in summer due to the summer monsoon. Indeed, the preindustrial summer minima observed at these two sites resemble the minima in present-day observations over Japan [*Thouret et al.*, 1998]. In Vienna the observations show a strong seasonal maximum, but the peak is shifted for unknown reasons toward summer. The other Northern Hemisphere sites have extremely weak spring maxima. Matching the weaker (or nearly nonexistent) observed springtime maxima in the model would require implementing a sink of ozone that operated mainly in late winter or early spring.

At Luanda, at 9°S, little influence from stratospheric ozone is expected. The observations show no seasonal cycle, while the model calculates a strong peak in August due to biomass burning. Here the mismatch between the model and the observations may point to our lack of knowledge of biomass burning in Africa during preindustrial times.

There is no pronounced interhemispheric difference in preindustrial ozone, either in the observations or in the standard model simulation (Figure 1). In the observations, the annual mean mixing ratio for the Southern Hemisphere midlatitude sites (11 ppb) is close to that of the Northern Hemisphere midlatitude surface sites (10 ppb). In the standard preindustrial simulation the annual mean mixing ratios for the midlatitude surface sites fall between 15 and 18 ppb, with no interhemispheric differences apparent. This lack of interhemispheric gradient in the preindustrial model is due to the absence of Northern Hemisphere pollution and the dependence of midlatitude ozone on chemical production in the tropics, which is nearly symmetric with respect to the equator.

Finally, the vertical gradient of preindustrial ozone can be inferred by comparing observations at the two mountain sites to observations at the surface. Curiously, the observations at Pic du Midi and Mont Ventoux in the free troposphere exhibit ozone levels equivalent to or only a couple parts per billion greater than the observed levels at the nearby surface sites of Coimbra, Vienna, and Montsouris. In all our preindustrial simulations, ozone mixing ratios increase from the surface to the free troposphere due to net loss in the boundary layer (Figure 4). Such a gradient is also a standard feature of present-day observations in remote regions. As mentioned above, the Montsouris data were filtered in the *Volz and Kley* [1988] analysis to exclude observations made when the wind blew across Paris or when wind speeds were less than 1 km h^{-1}. In another analysis of the Montsouris data [*Anfossi et al.*, 1991], all data were considered, yielding an annual mean ozone of only 7 ppb, compared to 9 ppb in the *Volz and Kley* [1988] study. Comparing the *Anfossi et al.* [1991] observations at Montsouris to the observations at Pic du Midi and Mont Ventoux yields a slightly greater vertical gradient of 3-5 ppb. Reducing the vertical gradient of ozone in the model to these values would require adding a high-altitude sink of ozone.

In summary, the ensemble of preindustrial observations show spatial and seasonal variations that are in part consistent with current understanding of the natural ozone budget (monsoonal summer minimum in Asia, lack of interhemispheric gradient) and in part inconsistent (weak or absent spring maximum, lack of gradient from the surface to the free troposphere).

7. Conclusions

Simulations with a global three-dimensional model of tropospheric chemistry suggest that uncertainties in the preindustrial, natural emissions of NO_x and hydrocarbons might accommodate decreases of preindustrial ozone concentrations by 10-20 ppb relative to the values in standard models used for radiative forcing calculations. These lower concentrations better match the observations made at surface and mountain sites at the turn of the nineteenth century. Concern remains over calibration of these nineteenth century measurements.

For the simulations that best matched the preindustrial observations (test cases 1 and 2), soil NO_x emissions were halved relative to the standard simulation to 2.0 Tg N yr^{-1}; biogenic emissions of isoprene, alkenes, and acetone were increased by 50%; monoterpene emissions were added; and lightning NO_x emissions were decreased to 1.0 or 2.0 Tg N yr^{-1} from 3.6 Tg N yr^{-1}. These test simulations represent our best reconstructions of the global preindustrial ozone fields constrained by the 1870-1910 surface air observations. Summertime concentrations at northern midlatitude sites (e.g., Montsouris) in the preindustrial simulation are most

sensitive to changes in biogenic sources, but bringing the wintertime concentrations in accord with the observations requires in addition a decrease of the lightning source in the tropics. The spring maximum of ozone, which is a prominent feature of the present-day climatology [*Logan et al.*, 1981], is weak or absent in the 1870-1910 observations. The model shows a strong spring maximum in all preindustrial simulation cases, reflecting transport from the stratosphere and the long lifetime of ozone in winter. Based on current understanding, it is not clear how one could suppress the spring ozone maximum in models of the preindustrial atmosphere.

Test cases 1 and 2 yield a global mean radiative forcing from ozone added to the atmosphere since preindustrial times of 0.72-0.80 W m^{-2}, well outside the range of forcings (0.3-0.5 W m^{-2}) obtained by standard models [*Ramaswamy*, 2001].

Uncertainties in calibration of the 1870-1910 measurements must be acknowledged, and could in the end account for the discrepancy with the standard preindustrial models. However, as shown here, uncertainties in the preindustrial sources of NO_x and hydrocarbons could also account for the discrepancy. By using our model to generate global distributions of ozone in the preindustrial atmosphere that match the constraints offered by the surface observations, we find that tropospheric ozone may have contributed a much larger fraction of total greenhouse forcing since preindustrial times than is generally assumed. This result points to the need for better understanding of the factors controlling natural sources of NO_x and hydrocarbons to the atmosphere and their trends.

References

Anfossi, D., S. Sandroni, and S. Viarengo, Tropospheric ozone in the nineteenth century: The Moncalieri series, *J. Geophys. Res., 96,* 17,349-17,352, 1991.

Bey, I., Contribution des processus nocturnes à la chemie troposphérique: Modélisation des flux de radicaux et transformation des précurseurs d'ozone (COV, NO$_x$), Ph. D. thesis, 253 pp., Univ. of Paris, Paris, May 1997.

Bojkov, R. D., Surface ozone during the second half of the nineteenth century, *J. Clim. Appl. Meteorol., 25,* 343-352, 1986.

Brasseur, G. P., J. Kiehl, J. F. Müller, T. Schneider, C. Granier, X. Tie, and D. Hauglustaine, Past and future changes in global tropospheric ozone: Impact on radiative forcing, *Geophys. Res. Lett., 25,* 3807-3810, 1998a.

Brasseur, G. P., D. A. Hauglustaine, S. Walters, P. J. Rasch, J.-F. Müller, C. Granier, and X. X. Tie, MOZART, a global chemical transport model for ozone and related chemical tracers, 1, Model description, *J. Geophys. Res., 103,* 28,265-28,289, 1998b.

Davidson, E. A., and W. Kingerlee, A global inventory of

nitric oxide emissions from soils, *Nutrient Cycling Agroecosyst. 48,* 37-50, 1997.

De Gouw, J. A., and E. R. Lovejoy, Reactive uptake of ozone by liquid organic compounds, *Geophys. Res. Lett., 25,* 931-934, 1998.

Granier, C., G. Pétron, J.-F. Müller, and G. Brasseur, The impact of natural and anthropogenic hydrocarbons on the tropospheric budget of carbonmonoxide, *Atmos. Environ., 34,* 5255-5270, 2000.

Griffin, R. J., D. R. Cocker III, J. H. Seinfeld, and D. Dabdub, Estimate of global atmospheric organic aerosol from oxidation of biogenic hydrocarbons, *Geophys. Res. Lett., 26,* 2721-2724, 1999.

Guenther, A., et al., A global model of natural volatile organic compound emissions, *J. Geophys. Res., 100,* 8873-8892, 1995.

Hansen, J., G. Russell, D. Rind, P. Stone, A. Lacis, S. Lebedeff, R. Ruedy, and L. Travis, Efficient three-dimensional models for climate studies: Models I and II, *Mon. Weather Rev., 3,* 609-662, 1983.

Hauglustaine, D. A., G. P. Brasseur, S. Walters, P. J. Rasch, J. F. Müller, L. K. Emmons, and M. A. Carroll, MOZART: A global chemical transport model for ozone and related chemical tracers, 2, Model results and evaluation, *J. Geophys. Res., 103,* 28,291-28,335, 1998.

Horowitz, L. W., J. Liang, G. M. Gardner, and D. J. Jacob, Export of reactive nitrogen from North America during summertime: Sensitivity to hydrocarbon chemistry, *J. Geophys. Res., 103,* 13,451-13,476, 1998.

Houghton, J. T., B. A. Callander, and S. K. Varney, *Climate Change 1992: The Supplementary Report to the IPCC Scientific Assessment,* 200 pp., Cambridge Univ. Press, New York, 1992.

Huntreiser, H., H. Schlager, C. Feigl, and H. Höller, Transport and production of NO_x in electrified thunderstorms: Survey of previous studies and new observations at midlatitudes, *J. Geophys. Res., 103,* 28,247-28,264, 1998.

Jacob, D. J., and S. C. Wofsy, Photochemistry of biogenic emissions over the Amazon forest, *J. Geophys. Res., 93,* 1477-1486, 1988.

Kiehl, J. T., T. Schneider, R. Portmann, and S. Solomon, Climate forcing due to tropospheric and stratospheric ozone, *J. Geophys. Res., 104,* 31,239-31,254, 1999.

Kley, D., A. Volz, and F. Mülheims, Ozone measurements in historic perspective, in *Tropospheric Ozone: Regional and Global Scale Interactions,* edited by I. S. A. Isaksen, pp 63-72, D. Reidel, Norwell, Mass., 1988.

Koch, D., D. Jacob, I. Tegen, D. Rind, and M. Chin, Tropospheric sulfur simulation and sulfate direct radiative forcing in the GISS GCM, *J. Geophys. Res., 104,* 23,799-23,822, 1999.

Lawrence, M. G., and P. J. Crutzen, The impact of cloud particle gravitation settling on soluble trace gas distributions, *Tellus, 50B,* 263-289, 1998.

Lawrence M. G., P. J. Crutzen, P. J. Rasch, B. E. Eaton, and N. M. Mahowald, A model for studies of tropospheric photochemistry: Description, global distributions, and evaluation, *J. Geophys. Res., 104,* 26,245-26,277, 1999.

Levy, H., II, W. J. Moxim, and P. S. Kasibhatla, A global three-dimensional time-dependent lightning source of NO_x, *J. Geophys. Res., 101,* 22,911-22,922, 1996.

Logan, J. A., Ozone in rural areas of the United States, *J. Geophys. Res., 94,* 8511-8532, 1989.

Logan, J. A., M. J. Prather, W. C. Wofsy, and M. B. McElroy, Tropospheric chemistry: a global perspective, *J. Geophys. Res., 86,* 7210-7254, 1981.

Lyons, W. A., T. E. Nelson, E. R. Williams, J. A. Cramer, and T. R. Turner, Enhanced positive cloud-to-ground

lightning in thunderstorms ingesting smoke from fires, *Science*, *282*, 77–80, 1998.

Marenco, A., H. Gouget, P. Nédélec, J. P. Pagés, and F. Karcher, Evidence of a long-term increase in tropospheric ozone from Pic du Midi data series: Consequences: Positive radiative forcing, *J. Geophys. Res.*, *99*, 16,617–16,632, 1994.

Mather, A. S., J. Fairbairn, and C. L. Needle, The course and drivers of the forest transition: The case of France, *J. Rural Stud.*, *15*, 65–90, 1999.

McLinden, C. A., S. Olsen, B. Hannegan, O. Wild, M. J. Prather, and J. Sundet, Stratospheric ozone in 3-D models: A simple chemistry and the cross-tropopause flux, *J. Geophys. Res.*, *105*, 24,653–14,665, 2000.

Mickley, L. J., P. P. Murti, D. J. Jacob, J. A. Logan, D. M. Koch, and D. Rind, Radiative forcing from tropospheric ozone calculated with a unified chemistry-climate model, *J. Geophys. Res.*, *104*, 30,153–30,172, 1999.

Palo, M., No end to deforestation?, in *World Forests, Society and Environment*, edited by M. Palo and J. Uusivuori, pp. 65–77, Kluwer Acad., Norwell, Mass., 1999.

Pavelin, E. G., C. E. Johnson, S. Rughooputh, and R. Toumi, Evaluation of pre-industrial surface ozone measurements made using the Schönbein method, *Atmos. Environ.*, *33*, 919–929, 1999.

Penner, J. E., Carbonaceous aerosols influencing atmospheric radiation: Black and organic carbon, in *Aerosol Forcing of Climate*, edited by R. J. Charlson and J. Heintzenberg, pp. 91–108, John Wiley, New York, 1995.

Prather, M., and D. Ehhalt, Atmospheric chemistry and greenhouse gases, in *Climate Change: The Scientific Basis, The IPCC Working Group 1 Third Assessment Report*. Cambridge Univ. Press, New York, in press, 2001.

Price, C., and D. Rind, A simple lightning parameterization for calculating global lightning distributions, *J. Geophys. Res.*, *97*, 9919–9933, 1992.

Price, C., and D. Rind, Possible implications of global climate change on global lightning distributions and frequencies, *J. Geophys. Res.*, *99*, 10,823-10,831, 1994.

Price, C., J. Penner, and M. Prather, NO_x from lightning, 1, Global distribution based on lightning physics, *J. Geophys. Res.*, *102*, 5929–5941, 1997.

Ramaswamy, V., Radiative forcing of climate change, in *Climate Change: The Scientific Basis, The IPCC Working Group 1 Third Assessment Report*. Cambridge Univ. Press, New York, in press, 2001.

Rind, D., and J. Lerner, Use of on-line tracers as a diagnostic tool in general circulation model development, 1, Horizontal and vertical transport in the troposphere, *J. Geophys. Res.*, *101*, 12,667–12,683, 1996.

Rind, D., J. Lerner, K. Shah, and R. Suozzo, Use of on-line

tracers as a diagnostic tool in general circulation model development, 2, Transport between the troposphere and the stratosphere, *J. Geophys. Res.*, *104*, 9123–9139, 1999.

Roelofs, G. J., J. Lelieveld, and R. van Dorland, A three-dimensional chemistry/general circulation model simulation of anthropogenically derived ozone in the troposphere and its radiative forcing, *J. Geophys. Res.*, *102*, 23,389–23,401, 1997.

Thouret, V., A. Marenco, J. A. Logan, P. Nédélec, and C. Grouhel, Comparisons of ozone measurements from the MOZAIC airborne program and the ozone sounding network at eight locations, *J. Geophys. Res.*, *103*, 25,695–25720, 1998.

Vitousek, P. M., J. D. Aber, R. W. Howarth, G. E. Likens, P. A. Matson, D. W. Schindler, W. H. Schlesinger, and D. G. Tilman, Human alteration of the global nitrogen cycle: Sources and consequences, *Ecol. Appl.*, *7*, 737–750, 1997.

Volz, A., and D. Kley, Evaluation of the Montsouris series of ozone measurements made in the nineteenth century, *Nature*, *332*, 240–242, 1988.

Wang, Y., and D. J. Jacob, Anthropogenic forcing on tropospheric ozone and OH since preindustrial times, *J. Geophys. Res.*, *103*, 31,123–31,135, 1998.

Wang, Y., D. J. Jacob, and J. A. Logan, Global simulation of tropospheric O_3-NO_x-hydrocarbon chemistry, 1, Model formulation, *J. Geophys. Res.*, *103*, 10,713–10,725, 1998a.

Wang. Y., D. J. Jacob, and J. A. Logan. Global simulation of tropospheric O_3-NO_x-hydrocarbon chemistry, 2, Model evaluation and global ozone budget, *J. Geophys. Res.*, *103*, 10,727–10,755, 1998b.

Westcott, N. E., Summertime cloud-to-ground lightning activity around major midwestern urban areas, *J. Appl. Meteorol.*, *34*, 1633–1642, 1995.

Williams, E. J., J. M. Roberts, K. Baumann, S. Buhr, R. B. Norton, and F. C. Fehsenfeld, Variations in NO_y composition at Idaho Hill, Colorado, *J. Geophys. Res.*, *102*, 6297–6314, 1997.

Yienger, J. J., and H. Levy II, Empirical model of global soil-biogenic NO_x emissions, *J. Geophys. Res.*, *100*, 11,447–11,464, 1995.

D. J. Jacob and L. J. Mickley, Division of Engineering and Applied Sciences and Department of Earth and Planetary Sciences, Harvard University, 29 Oxford St., Cambridge, MA 02138. (e-mail: ljm@io.harvard.edu)

D. Rind, Goddard Institute for Space Studies, 2880 Broadway, New York, NY 10025.